SAND2021-7530C

FRACTURE PROPERTIES OF WELDED 304L IN HYDROGEN ENVIRONMENTS

Ronevich, J.A.[1], San Marchi, C.[2], Maguire, M.[3], Balch, D.K.[4]
[1] Sandia National Laboratories, 7011 East Ave, Livermore CA, USA, jaronev@sandia.gov
[2] Sandia National Laboratories, 7011 East Ave, Livermore CA, USA, cwsanma@sandia.gov
[3] Sandia National Laboratories, 7011 East Ave, Livermore CA, USA, mcmagui@sandia.gov
[4] Sandia National Laboratories, 7011 East Ave, Livermore CA, USA, dkbalch@sandia.gov

ABSTRACT

Austenitic stainless steels are used for hydrogen containment of high-pressure hydrogen gas due to their ability to retain high fracture properties despite the degradation due to hydrogen. Forging and other strain-hardening processes are desirable for austenitic stainless steels to increase the material strength, and thus accommodate higher stresses and reduce material costs. Welding is often necessary for assembling components, but it represents an area of concern in pressure containment structures due to the potential for defects, more environmentally susceptible microstructure, and reduced strength. Electron beam (EB) welding represent an advanced joining process which has advantages over traditional arc welding techniques, through reduced input heat and reduced heat-affected zone (HAZ) microstructure, and thus present a means to maintain high strength and improve weld performance in hydrogen gas containment. In this study, fracture coupons were extracted from EB welds in forged 304L and subjected to thermal gaseous hydrogen precharging at select pressures to introduce different levels of internal hydrogen content. Fracture tests were then performed on hydrogen precharged coupons at temperatures of both 293 K and 223 K. It was observed that fracture resistance (J_H) was dependent on internal hydrogen concentration; higher hydrogen concentrations resulted in lower fracture resistance in both the forged 304L base material and the 304L EB welds. This trend was also apparent at both temperatures: 293 K and 223 K. EB weld samples, however, maintain high fracture resistance, comparable to the forged 304L base material. The role of weld microstructure solidification on fracture is discussed.

1.0 INTRODUCTION

Hydrogen degrades mechanical properties of most materials and although austenitic stainless steels are more resistant, mechanical properties such as ductility and fracture resistance are still reduced when internal hydrogen is present [1, 2]. Degradation due to hydrogen in austenitic stainless steels manifests itself as reductions in ductility or fracture resistance [1-3]. Evaluating hydrogen degradation of austenitic stainless steels is challenging as the diffusivity of hydrogen is extremely slow [4], therefore thermally precharging gaseous hydrogen into the material prior to mechanical testing has been adopted to ensure a uniform concentration [1, 2]. Significant work has been done on austenitic stainless steels [1, 2, 5-8]; however, less work has been done on welds [3, 9, 10]. Welds represent an area of concern because the welding process can introduce varying microstructures, residual stresses, and often times ferrite which has lower fracture resistance than austenite [3]. Beyond microstructural effects, the welds themselves can have defects or geometric discontinuities at weld joints which may serve as stress concentrators and crack nucleation sites; therefore, it is important to understand the mechanical response of stainless steel welds if they are being used in a hydrogen environment.

Previous work on 304L welds has shown that ferrite can degrade fracture resistance when fracture tests were performed on thermal hydrogen precharged gas tungsten arc (GTA) welds [10]. In general, fracture resistance and ductility of arc welds that have been thermally precharged with hydrogen have exhibited poorer performance than base metals [9, 10]. However, electron beam (EB) welding is typically autogenous, i.e. no filler metal added, and have characteristics that are superior to conventional GTA welding. EB welds are typically narrower than GTA welds and therefore have a faster cooling rate, finer microstructure and lower residual stresses. This all contributes to improved mechanical properties. Previous work examining tensile properties of 304L EB welds compared to

GTA welds shows superior behavior of the EB welds and comparable reduction of area measurements to the base metal [9].

In this study, forged 304L EB welds and forged 304L base metal were subjected to thermal hydrogen precharging to introduce two different internal hydrogen concentrations. Fracture resistance and reduction of area were measured at 293 K and 223 K to compare the resilience of EB welds to forged 304L.

2.0 EXPERIMENAL PROCEDURES

2.1 Materials

A metastable austenitic stainless steel, 304L, was the parent material used in this study. The material was tested in both the as-forged and welded condition. The forging condition is described in Ref. [2] which achieved a yield strength of 447 MPa and a tensile strength of 666 MPa in the circumferential direction of the forged cylinder. Rings were machined from forged cylinders that were subsequently circumferentially EB welded as described in Ref. [3]. The weld rings were nominally 81 mm in diameter and are shown in Fig. 1. For the EB weld evaluation, dog-bone type tensile coupons were removed from the welded rings with the EB weld centered in the gauge section as shown in Fig. 1. Similarly, GTA weld fracture coupons were removed such that the crack plane was centered in the weld region with the crack extending from inside to outside surface, i.e. the radial direction, and the loading axis was parallel to the tensile coupons as shown in Fig. 1, i.e. the longitudinal direction. Schematics of the tensile and GTA weld coupons are shown in Fig. 2. For evaluation of the as-forged 304L material, dog-bone tensile coupons and arc fracture coupons were removed from the cylindrical forging such that the loading axis was the circumferential direction. For the arc coupons, the crack growth direction was radial. Coupons were fatigue precracked to crack length (a/W) of approximately 0.5 prior to hydrogen-precharging.

The microstructure of the forged 304L and EB weld are quite different and are shown in Fig. 3. The 304L base metal shows large equiaxed austenite grains ranging from 20-30 microns as shown in Fig. 3a. The EB weld microstructure consists of skeletal ferrite (thin dark regions) in an austenite matrix (white). Ferrite content was measured in the welds using a Feritscope®. Ferrite contents increased from inner to outer diameter of the weld ring. An average ferrite number (FN) of 3.5 was measured at the mid-thickness of the weld which is relevant to the microstructure sampled during a fracture test. The EB weld has significantly finer features than the base metal. It should be noted that many of the dendritic features in the EB weld in Fig. 3b are in the longitudinal (L) direction, i.e. perpendicular to the crack propagation direction, which is radial (R). This is a result of the narrow width of the EB weld. During the welding process, the largest heat gradient is into the adjacent parent base metal in the longitudinal direction. The benefits of EB welding over more traditional arc welding are deeper/narrow welds, faster cooling rates and consequently finer microstructural features.

2.2 Hydrogen precharging

Tensile and arc fracture coupons were thermally precharged at 573 K in gaseous hydrogen for a minimum of 10 days to achieve a uniform hydrogen concentration. Precharging was conducted in batches at two different pressures: 138 MPa H_2 and 41 MPa H_2 in order to achieve uniquely different internal hydrogen concentrations based on estimates of solubility from Ref. [4]. Four different hydrogen measurements for the lower pressure condition (i.e. 41 MPa) were made at an external lab using inert gas fusion-infrared absorbance and the measured average value was 66 wt ppm. Previous work [3, 11] has shown that thermally precharging at 138 MPa results in approximately 140 wppm H. Following thermal precharging, coupons were stored in a freezer at 220 K until testing which ensures that minimal egress of hydrogen occurs during storage.

2.3 Tensile test measurements

Tensile coupons were tested on a servo-hydraulic load frame in air at two different temperatures: 293 K and 223 K. Tests were performed at a constant displacement rate of 1.27 mm/min and a 12.7 mm extensometer was used to measure strain. This displacement rate corresponds to a strain rate of approximately 5 x 10^{-4} s^{-1} within the extensometer gauge. The low temperature testing was accomplished by using an environmental chamber in-situ in the load train that was cooled by cryogenic nitrogen. The 223 K experiments were held at temperature for a minimum of 10 minutes before loading to ensure uniform temperatures through the coupon. The 0.2% offset yield strength, tensile strength, and reduction of area (RA) were calculated following the tests. Reduction of area (RA) was selected as the best metric for ductility rather than total elongation to failure as the limited width of the weld (< 2 mm) results in artificially lower elongation to failure in the EB welds compared to the base metals, as the majority of the deformation occurs in the lower strength weld region.

2.4 Fracture measurements

GTA weld fracture coupons were tested by constant rising displacement fracture toughness tests according to ASTM E1820 [12]. The GTA weld specimen geometry is described in ASTM E399 [13] but an elastic-plastic fracture analysis was performed according to ASTM E1820 [12]. Previous work [3, 14] showed that using this analysis [3, 14] with the GTA weld specimen yields similar fracture toughness values to more conventional compact tension specimens for austenitic stainless steels and pipeline steel welds. GTA weld fracture coupons were tested at 1.5 mm/hr and crack positions were monitored using direct current potential difference (DCPD) according to ASTM E1820 [12]. Following the test, crack extension was marked by heat tinting to 350°C for 1 hr followed by fatigue cycling to separate the remaining ligament and examine the fracture surface. J-R curves were generated from monitored load, displacement and DCPD values according to ASTM E1820 [12]. Fracture resistance (J_H) was determined by the intersection of the J-R curve with the 0.2 mm construction line. ASTM E1820 [12] allows for conversion of J values to equivalent linear-elastic K values according to equation 1 if certain validity criteria were met:

$$K_{JH} = \sqrt{\frac{EJ_H}{1-\nu^2}} \quad (1)$$

where E is elastic modulus (E=193 GPa), K_{JH} is the equivalent linear elastic fracture resistance calculated from J_H, ν is Poisson's ratio of 0.3. The validity criteria are described in equation 2 below:

$$B > 10J_Q/S_Y \text{ and } b_o > 10J_Q/S_Y \quad (2)$$

where B is thickness of the test coupon, S_Y is the flow stress, and b_o is the remaining uncracked ligament. Not all tests passed this validity criteria, particularly the low H-content results, therefore in order to facilitate comparisons within this study, the results are discussed on the basis of J_H.

2.5 Microscopy

Optical and electron microscopy were performed to examine the microstructures in the pre and post tested conditions. Scanning electron microscopy (SEM) images were taken using electron backscattered diffraction (EBSD) after the fracture tests were completed to examine the effects of grain orientation on crack growth. For comparison in the discussion section, microscopy was also performed on fracture coupons of a GTA welded 304L with 308L filler metal reported in ref [3]. This weld consists of predominantly austenite matrix with a long dendritic structure of skeletal ferrite. The solidification structure is mainly oriented parallel to the crack path of which the consequences will be discussed.

3.0 RESULTS

3.1 Tensile properties

Duplicate tensile tests were performed, and the average results are reported in Table 1 for the forging and Table 2 for the EB weld. In general, the strength properties, i.e. yield strength and tensile strength, increase with hydrogen content. However, the yield strength of the 304L forged decreases at 223 K compared to 293 K for each H-content, whereas the tensile strength increases. In comparison, the 304L EB weld shows an increase in both yield and tensile strengths with increasing hydrogen and with decreasing temperature. Ductility, as measured by reduction of area (RA), is reduced by increasing hydrogen content. This is consistent with Ref [1]. The reduction of area results are plotted in Fig. 4 as a function of wt ppm H. The reduction of area decreases for both the forged and EB welded 304L similarly at 293 K and 223 K; however, the RA for 223 K is reduced further in both materials. For reference the RA from Ref [1] is shown for the non-charged (i.e. 0 wt ppm H) condition at 293 K and 223 K for a forged 304L.

3.2 Fracture properties

The measured fracture resistance, J_H, in the hydrogen-precharged conditions are shown in Fig. 5 for the forged 304L and EB weld. Triplicate tests were done in all conditions except for the 304L EB weld at 66 wt ppm and 223 K. Table 3 summarizes the results of the individual fracture tests. Fracture tests in the non-charged condition did not exhibit crack extension and therefore a valid J_H value could not be obtained. The fracture resistance, J_H, for both the forged 304L and EB welds shows a dependency on H-concentration and temperature. In both materials, the J_H decreases with increasing H-content and decreasing temperature.

3.2.1 Forged 304L

For the forged 304L at 293 K, the average fracture resistance decreased from 390 to 270 kJ/m^2 for the 66 and 140 wt ppm H, respectively. The lower temperature experiments at 223 K resulted in average fracture resistance values of 159 and 82 kJ/m^2 for the 66 and 140 wt ppm H, respectively. The effects of temperature on J_H are apparent in that at 66 wt ppm results, the J_H decreases from 390 to 159 kJ/m^2 for 293 K and 223 K, respectively. Similarly, the higher hydrogen concentration of 140 wt ppm exhibits a decrease in J_H from 270 to 82 kJ/m^2 when temperature was decreased from 293 K to 223 K.

3.2.2 304L EB welds

The EB weld also exhibits a sizeable decrease in J_H when comparing changes in H-concentration and temperature. At 293 K, the average J_H results for 66 to 140 wt ppm were 424 and 216 kJ/m^2, respectively. The experiments at 223 K also showed H-concentration dependency with average values of 181 and 112 kJ/m^2 for the 66 to 140 wt ppm H conditions, respectively. With internal hydrogen contents of 66 wt ppm, the J_H dropped from 424 to 181 kJ/m^2 as the temperature was dropped from 293 K to 223 K. Similarly, at 140 wt ppm, the J_H decreased from 216 to 112 kJ/m^2 at temperatures of 293 K and 223 K, respectively.

4.0 DISCUSSION

4.1 Effects of Hydrogen Concentration

As demonstrated in this study, elevated internal hydrogen concentrations can have detrimental effects on mechanical properties of austenitic stainless steels and welds. The effects of internal precharged hydrogen content on reduction of area and fracture resistance is discussed.

4.1.1 Reduction of Area at Different H-concentrations

The decrease in reduction of area results are consistent with previous work [1] which measured RA in forged 304L tensile samples to be RA=0.85 (0 wt ppm H), RA=0.52 (50 wt ppm H), RA=0.43 (100 wt ppm H), and RA=0.40 (140 wt ppm H) at 293 K. In the present work, RA was measured to be RA=0.81 (0 wt ppm H), RA=0.53 (66 wt ppm H), RA=0.38 (140 wt ppm H) at 293 K. Similar trends were measured for the 223 K experiments between this work and previous [1] thermally precharged to comparable internal hydrogen concentrations for forged 304L. The results from [1] at 223 K at varying H-concentration were RA=0.81 (0 wt ppm H), RA=0.29 (50 wt ppm H), RA=0.21 (100 wt ppm H), and RA=0.19 (140 wt ppm). For the present study, tensile tests were performed on samples precharged to 66 and 140 wt ppm H and tested at 223 K, which had RA = 0.30 and 0.21, respectively.

Electron-beam welds also exhibited a significant decrease in RA with increasing H-concentration with measured RA=0.9 (0 wt ppm H) to RA=0.53 (66 wt ppm H) to RA=0.42 at 140 wt ppm H at 293 K. A comparison of the results at 223 K between the two levels of H-concentration showed a similar trend with increasing H-content albeit the RA were lower than at 293 K. For the tensile tests measured at 223 K with internal hydrogen contents of 66 and 140 wt ppm H, the measured RA = 0.25 and 0.22, respectively. Work by Younes [9] on EB welded 304L tested at room temperature showed comparable RA values for similar H-contents (e.g. RA=0.47 for 57 wt ppm H). However, with 0 and 160 wt ppm H, in Younes work [9] the RA was 0.59 and 0.29, respectively which are much lower than in the present study. Overall the RA values from Younes study [9] were lower than in the present study.

From these results, it is clear that hydrogen content degrades the RA in both forged 304L and EB welds as shown in Fig. 4. However, the trend does not appear to be linear from 0 to 140 wt ppm H. The largest drop in RA appears to take place at the lower H-content (i.e. 66 wt ppm) and then RA gradually decreases up to 140 wt ppm. A linear trend of decreasing RA was measured in Ref [1] for both 304L and 316L between 50 and 140 wt ppm H, but between 0 and 50 wt ppm, the slope was steeper much like in the present study. The EB weld and forged 304L follow this similar behavior although the magnitude may be larger due to temperature as will be discussed in Section 4.2.1.

4.1.2 Reduction in Fracture Resistance at Different H-concentration

Degradation of fracture resistance due to hydrogen content is clearly evident in Figure 5 for the forged 304L. As mentioned previously, fracture tests in the non-charged condition did not exhibit any measurable crack extension and therefore J_H values were not calculated. At 293 K, triplicate measurements of the forged 304L precharged with 66 wt ppm H had an average J_H of 390 kJ/m^2 which decreased to 270 kJ/m^2 when the H-concentration was 140 wt ppm. This represents a decrease of 31%. For the EB weld, the fracture resistance reduced from 424 to 216 kJ/m^2 by increasing the internal hydrogen content from 66 to 140 wt ppm, respectively, which is a reduction of 49%. This decrease in the EB weld J_H is larger than in the forged 304L due to the very high J_H (i.e. 536 kJ/m^2) measured of the 3rd test of the EB weld at 66 wt ppm H 293 K measurement which shifted the average to a higher value.

At 223 K, the fracture resistance also degraded with increasing hydrogen content for both the forged 304L and EB weld. The J_H of the forged 304L decreased 48% from 159 to 82 kJ/m^2 with internal hydrogen contents of 66 and 140 wt ppm H, respectively. Similarly, the J_H of the EB weld decreased 38% from 181 to 112 kJ/m^2 with internal hydrogen contents of 66 and 140 wt ppm H, respectively.

4.2 Effects of Temperature

4.2.1 Reduction of Area at Different Temperatures

A comparison of the RA as a function of temperature for the same H-concentrations in Fig. 4 reveals that temperature has a significant influence. Tensile tests were not performed on the non-charged (i.e. 0 wt ppm H) condition at 223 K, however based on previous work [1], the RA was minimally reduced from 0.85 to 0.81 from 293 to 223 K for a forged 304L steel. In the present study, for the forged 304L

tensile samples tested with 66 wt ppm H, the RA is reduced from 0.53 to 0.30 for temperatures of 293 K and 223 K, respectively. Similarly, at 140 wt ppm H, the RA reduces from 0.38 to 0.21 for 293 K and 223 K tests, respectively.

The EB welds exhibit similar decreasing trends in RA with temperature where at 66 wt ppm H, the RA reduces over 50% from 0.53 to 0.25 for tests at 293 K and 223 K, respectively. At the higher H-concentration of 140 wt ppm H, the RA is reduced from 0.42 to 0.22 at temperatures of 293 K and 223 K.

As previous work showed [1], without any hydrogen the RA changes negligibly from 293 K to 223 K; however, once hydrogen is present in the material the RA drops significantly at low temperature. Furthermore, it appears that the EB weld may be more sensitive to temperature than the forged 304L as the RA is more severely degraded. With hydrogen present (e.g. at 66 and 140 wt ppm H), the decrease in RA due to temperature decreased on average by 50% in the EB weld compared to about 44% in the forged 304L. Although this in not a substantial difference it might be explained by the presence of ferrite in the EB weld which has an average ferrite content of 3.5%, whereas the forged 304L had negligible ferrite. Previous work [3] showed that below 8% ferrite, no real trends were observed between RA and ferrite content for hydrogen precharged tensile samples tested at 293 K, suggesting that at 293 K the presence of ferrite does not greatly reduce RA. Ferrite is more sensitive to temperature than austenite which may account for the reduced RA at 223 K in the EB weld. Additionally, metastable austenitic stainless steels, like 304L, are known to transform to martensite during low temperature deformation [1, 8]. Forged 304L with internal hydrogen contents from 0 to 140 wt ppm formed less than 3% martensite in the uniformly deformed gauge section when tested at 293 K [1]. This same material when tested at 293 K formed martensite contents up to 70% and also had correspondingly lower RA [1]. Previous work on austenitic stainless steels [8] showed that ductility was more degraded on metastable alloys such as 304L compared to more stable alloys such as 310 due to the potential to form martensite at lower temperatures in metastable alloys, which is more susceptible to low temperature embrittlement. In the present study, ferrite measurements of the uniformly deformed region were not possible on the EB weld as the entire weld region exhibited non-uniform deformation as a result of it being lower strength than the base metal. However, it is likely that both formed significant amounts of martensite at 223 K resulting in low temperature embrittlement which further reduced the RA. Because the EB weld started with 3.5% ferrite, the susceptibility to low temperature embrittlement was perhaps slightly greater than the forged 304L, which lead to the lower RA values of the EB weld at 223 K.

4.2.2 Reduction of Fracture Resistance at Different Temperatures

The average fracture resistance of the forged 304L at 66 wt ppm H was 390 and 159 kJ/m^2 for 293 K and 223 K, respectively, which is a 59% decrease in J_H. Similarly, at 140 wt ppm, the forged 304L fracture resistance decreased from 270 to 82 kJ/m^2 when the temperature was decreased from 293 K to 223 K, respectively, which represents a 69% decrease. For the EB welds, the fracture resistance at 66 wt ppm H decreased 57% from 424 to 181 kJ/m^2 for temperatures at 293 K and 223 K, respectively. At 140 wt ppm H, the J_H for the EB welds decreased 48% from 216 to 112 kJ/m^2 when the temperature was dropped from 293 K to 223 K. These results show nearly a 50% or greater reduction in J_H when tested at sub-ambient temperatures of 223 K, for either of the internal H-contents examined. Similar to the discussion of temperature effects on RA, the fracture resistance appears to be sensitive to temperature regardless of whether the material is a weld or forging. Results from [3, 11] which examined a GTA welded 304L with 308L filler metal showed negligible differences in J_H at the two temperatures of interest (i.e. 293 K and 223 K) when precharged to 140 wt ppm H. However, the J_H values were between 120 and 130 kJ/m^2 [3, 11] at both temperatures indicating that the overall fracture resistance at 293 K was lower than the EB welds tested in the present study.

4.3 Comparison of Welds and Forged 304L

The average fracture resistance for the forged 304L and EB welds were 390 and 424 kJ/m^2 for 66 wt ppm H and 270 and 216 kJ/m^2 for 140 wt ppm H, respectively for tests at 293 K. It is worth noting that

the average of 424 kJ/m^2 for the EB weld is heavily influenced by the one high J_H measured value of 536 kJ/m^2 as shown in Table 3. If this value was excluded, the average of the other two 66 wt ppm H fracture tests would be 368 kJ/m^2. This, compared to the forged 304L value of 390 kJ/m^2, appears to be more consistent with the behavior of the 140 wt ppm H trend which is that the forged 304L has slightly higher J_H compared to the EB weld. Previous work [3] that looked at a variety of stainless steel base metals and compared to GTA welds showed that in general base metals outperform the welds in the hydrogen precharged condition at room temperature, but that amount varies from weld to weld. Two GTA welds of 304L with 308L filler metal [3, 11] (referred to as 304L/308L) tested at 293 K with 140 wt ppm H had fracture resistance values of 124 and 119 kJ/m^2. These weld J_H values are substantially lower than the EB weld presented in this study of 216 kJ/m^2. It is thought that the finer microstructure of the weld and the orientation of the solidification direction improves the fracture resistance of the EB weld [3]. Figure 6 shows electron backscattered diffraction (EBSD) images of a post-test fracture coupon of the EB weld with 140 wt ppm H tested at 293 K and 223 K. Focusing first on the image from the test at 293 K in Fig. 6, it is clear that the bulk grain orientation is perpendicular to the crack growth direction. This appears to result in crack tip branching and blunting in the fracture test at 293 K, which shows a very wide crack and multiple smaller regions where it is apparent that the crack branched. This can be compared to Fig. 7 for 304L/308L GTA weld tested at 293 K with 140 wt ppm H which was tested in Ref [3]. In Fig. 7a, the 304L/308L GTA weld microstructure consists of austenite (white) with skeletal ferrite microstructure (dark). The 304L/308L fracture coupons were removed such that the crack propagated in the radial direction in the center of the gas tungsten are weld [3]. This is parallel to the solidification direction in the GTA weld in the radial direction as shown in Fig. 7a. The overall weld size is much larger than the EB weld which contributes to slower cooler and coarser microstructure. Furthermore, a larger portion of the solidification structure is in the radial direction compared to the EB weld as shown in Fig. 3b and Fig. 6. EBSD images were captured on one of the fractured samples from Ref [3] as shown in Fig. 7b. The 304L/308L weld fracture coupon was oriented in the same direction as the EB weld where the crack growth direction is in the radial direction. It is clear that the crack easily follows the dendritic structure in the 304L/308L weld in Fig. 7b, whereas in the EB weld in Fig. 6, the crack deflects due to the solidification structure being predominantly perpendicular to the crack growth direction. The benefit of crack branching and blunting is higher fracture resistance (J_H = 216 kJ/m^2) which was measured in the EB weld at 293 K, compared to the 304L/308L which showed no indication of crack branching as the crack grew parallel to the solidification structure and had a J_H = 124 kJ/m^2.

A slightly different result was found when comparing the fracture behavior at low temperatures. At low temperatures (e.g. 223 K), the J_H for the forged 304L and EB welds were measured to be 159 and 181 kJ/m^2 for 66 wt ppm H, and for the forged 304L and EB welds the J_H values were 82 and 112 kJ/m^2 for 140 wt ppm H. These results show that the EB weld consistently exhibited higher fracture resistance at 223 K compared to the forged 304L, which is contrary to the trend at 293 K, which favored the forged 304L. Other low temperature (i.e. 223 K) fracture resistance measurements in the literature [3, 11] at 140 wt ppm H recorded J_H values of 119 and 125 kJ/m^2 for two different 304L/308L GTA welds, which is consistent with the 112 kJ/m^2 value of the EB in the present study. Figure 6b shows the crack profile of EB weld tested with 140 wt ppm H at 223 K. Although a clear crack deflection is observed in the crack profile, the amount of blunting (i.e. width of crack) is drastically reduced compared to the test at 293 K in Fig. 6a. The reduction in blunting is consistent with the lower fracture resistance value of 112 kJ/m^2. The low temperature fracture behavior appears to lower the fracture resistance of all the welds to a similar range of J_H, regardless of microstructure. However, the crack deflections are still present in the EB weld at 223 K which helps contribute to higher fracture resistance relative to the forged 304L.

The reduction of area between the forged 304L and EB welds were very similar with RA=0.81 and 0.9 for 0 wt ppm H, 0.53 and 0.53 for 66 wt ppm H, and 0.38 and 0.42 for 140 wt ppm H for the forged 304L and EB weld, respectively for tests at 293 K. The low temperature tests at 223 K show a similar trend with RA values of 0.30 and 0.25 for 66 wt ppm H and 0.21 and 0.22 for 144 wt ppm H, for the forged 304L and EB weld, respectively. The trends of this forged 304L is consistent with the literature [1]. The EB weld tested in this study exhibited comparable RA values to the forgings and better RA compared to other 304L welds from the literature as described in Younes [9].

Overall, the mechanical performance as measured by reduction of area and fracture resistance is comparable between the forged 304L and EB weld with 2 different internal hydrogen contents tested at 293 K and 223 K. The RA between the forged 304L and EB weld degraded similarly with increasing H-content and lower temperatures. Fracture resistance values were higher at 223 K for the EB weld, but slightly lower at 293 K; however, overall the two materials retained comparable fracture resistance.

5.0 CONCLUSIONS

Tensile and GTA fracture coupons extracted from forged 304L and 304L EB welds were thermally precharged with hydrogen at two different pressures to obtain approximately 66 and 140 wt ppm H. Tensile tests and rising displacement fracture tests were performed in air at 293 K and 223 K to evaluate the mechanical property degradation due to internal hydrogen concentration and temperature. Overall, the behavior of the EB weld is comparable to the forged 304L when assessing the mechanical properties of the fracture resistance and reduction of area influenced by internal hydrogen content and low temperature.

- At 293 K, forged 304L and EB weld exhibited a large decrease in RA with 66 wt ppm H which decreased further at 140 wt ppm H. The relationship was non-linear and showed a steeper drop from 0 to 66 wt ppm H compared to 66 wt ppm to 140 wt ppm H. More substantial decreases in RA were measured in both H-contents when tested at 223 K.

- Measured fracture resistance, J_H, scaled with internal hydrogen content for both forged 304L and EB weld. Fracture resistance decreased from 31% to 49% when comparing only the influence of H-content from 66 to 140 wt ppm H.

- When comparing the effects of temperature and at constant H-contents (e.g. either at 66 or 140 wt ppm H), the fracture resistance, J_H, dropped anywhere from 48% to 69% when the temperature was dropped from 293 K to 223 K.

- At 293 K, the J_H values of the forged 304L was slightly better than the EB weld, however at 223 K, the J_H values of the EB weld retained higher J_H at both H-contents. EBSD images of crack branching and blunting were observed to occur due to orientation of microstructure with respect to the crack growth direction in the EB weld at 293 K which likely contributed to the overall higher fracture resistance.

ACKNOWLEDGEMENTS

Sandia National Laboratories is a multimission laboratory managed and operated by National Technology and Engineering Solutions of Sandia, LLC., a wholly owned subsidiary of Honeywell International, Inc., for the U.S. Department of Energy's National Nuclear Security Administration under contract DE-NA-0003525.

REFERENCES

[1] C. San Marchi, J. A. Ronevich, J. E. C. Sabisch, J. D. Sugar, D. L. Medlin, and B. P. Somerday, "Effect of microstructural and environmental variables on ductility of austenitic stainless steels," *International Journal of Hydrogen Energy,* vol. 46, no. 23, pp. 12338-12347, 2021/03/31/ 2021, doi: https://doi.org/10.1016/j.ijhydene.2020.09.069.

[2] H. Jackson, C. San Marchi, D. Balch, B. Somerday, and J. Michael, "Effects of Low Temperature on Hydrogen-Assisted Crack Growth in Forged 304L Austenitic Stainless Steel," *Metallurgical and Materials Transactions A,* journal article vol. 47, no. 8, pp. 4334-4350, August 01 2016, doi: 10.1007/s11661-016-3563-y.

[3] J. Ronevich, C. San Marchi, and D. K. Balch, "Evaluating the resistance of austenitic stainless steel welds to hydrogen embrittlement, PVP2019-93823," presented at the ASME 2019 Pressure Vessels & Piping Conference, San Antonio, TX, 2019.

[4] C. W. San Marchi, B. P. Somerday, and S. L. Robinson, "Permeability, solubility and diffusivity of hydrogen isotopes in stainless steels at high gas pressures," *International Journal of Hydrogen Energy,* vol. 32, no. 1, pp. 100-116, 2007, doi: 10.1016/j.ijhydene.2006.05.008.

[5] C. S. Marchi and B. P. Somerday, "Comparison of stainless steels for high-pressure hydrogen service PVP2014-28811," presented at the ASME Pressure Vessels and Piping Division Conference, Anaheim, CA, 2014.

[6] C. San Marchi, T. Michler, K. A. Nibur, and B. P. Somerday, "On the physical differences between tensile testing of type 304 and 316 austenitic stainless steels with internal hydrogen and in external hydrogen," *International Journal of Hydrogen Energy,* vol. 35, no. 18, pp. 9736-9745, 2010, doi: 10.1016/j.ijhydene.2010.06.018.

[7] K. A. Nibur, B. P. Somerday, D. K. Balch, and C. San Marchi, "The role of localized deformation in hydrogen-assisted crack propagation in 21Cr–6Ni–9Mn stainless steel," *Acta Materialia,* vol. 57, no. 13, pp. 3795-3809, 2009, doi: 10.1016/j.actamat.2009.04.027.

[8] G. R. Caskey Jr, *Hydrogen compatibility handbook for stainless steels*, 1983.

[9] C. M. Younes, A. M. Steele, J. A. Nicholson, and C. J. Barnett, "Influence of hydrogen content on the tensile properties and fracture of austenitic stainless steel welds," *International Journal of Hydrogen Energy,* vol. 38, no. 11, pp. 4864-4876, 2013/04/15/ 2013, doi: https://doi.org/10.1016/j.ijhydene.2012.11.016.

[10] H. F. Jackson, K. A. Nibur, C. San Marchi, J. D. Puskar, and B. P. Somerday, "Hydrogen-assisted crack propagation in 304L/308L and 21Cr–6Ni–9Mn/308L austenitic stainless steel fusion welds," *Corrosion Science,* vol. 60, no. 0, pp. 136-144, 2012, doi: http://dx.doi.org/10.1016/j.corsci.2012.03.046.

[11] H. F. Jackson, C. San Marchi, D. K. Balch, and B. P. Somerday, "Effect of low temperature on hydrogen-assisted crack propagation in 304L/308L austenitic stainless steel fusion welds," *Corrosion Science,* vol. 77, no. 0, pp. 210-221, 2013, doi: http://dx.doi.org/10.1016/j.corsci.2013.08.004.

[12] *E1820-18a Standard Test Method for Measurement of Fracture Toughness*, ASTM, West Conshohocken, PA, 2018.

[13] *E399 Standard Test Method for Linear-Elastic Plane-Strain Fracture Toughness K_{IC} of Metallic Materials*, ASTM, West Conshohocken, PA, 2020.

[14] J. A. Ronevich, E. J. Song, B. P. Somerday, and C. W. San Marchi, "Hydrogen-assisted fracture resistance of pipeline welds in gaseous hydrogen," *International Journal of Hydrogen Energy,* vol. 46, no. 10, pp. 7601-7614, 2021/02/08/ 2021, doi: https://doi.org/10.1016/j.ijhydene.2020.11.239.

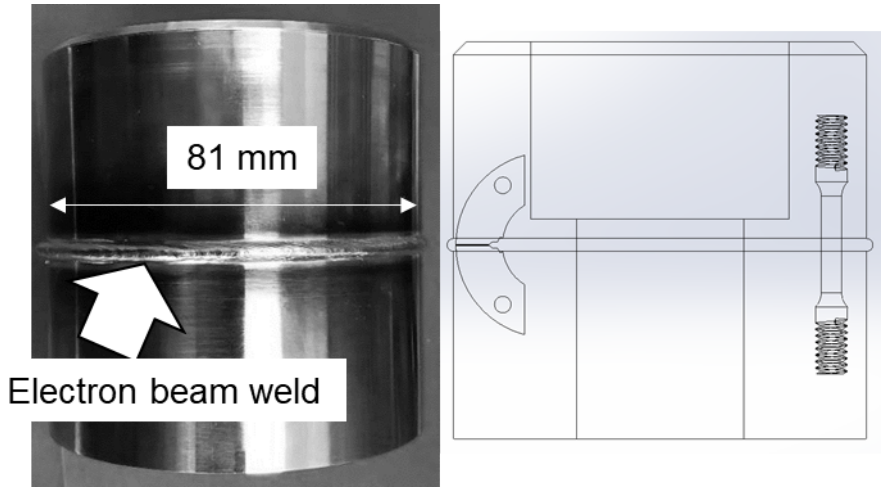

Figure 1. Electron beam weld ring with schematic showing approximate location of arc fracture and tensile coupons.

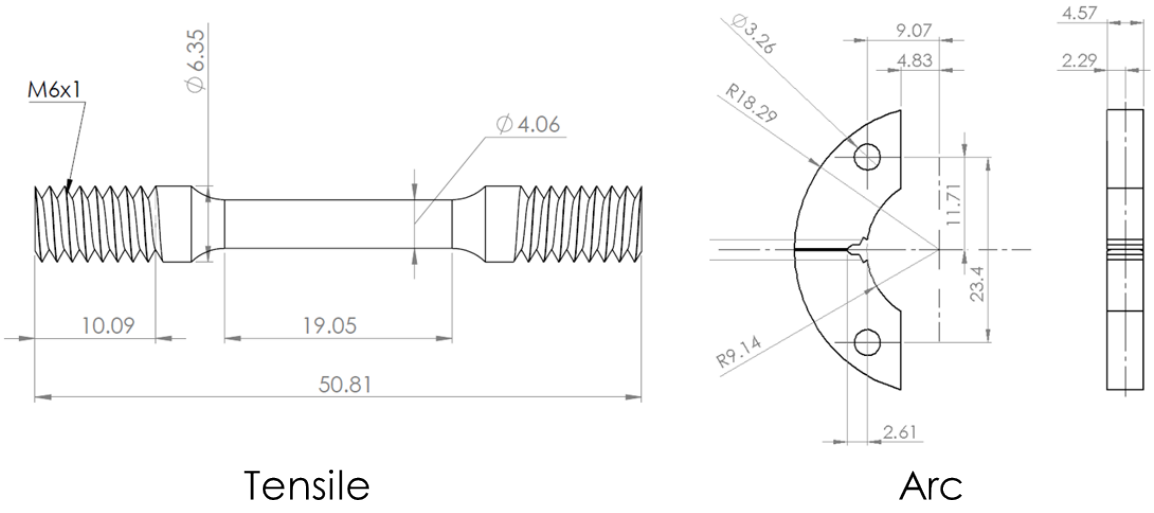

Figure 2. Dimensions (in mm) of tensile and arc fracture coupon used in this study.

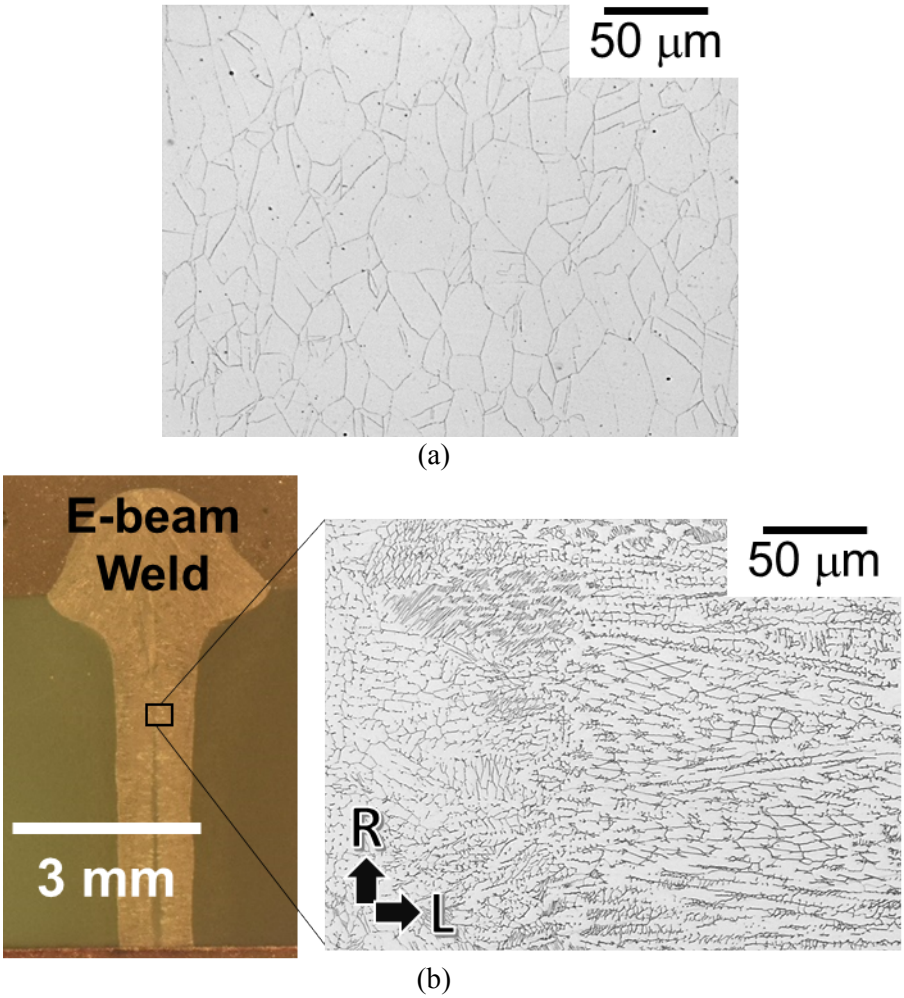

Figure 3. Optical images of (a) 304L forged base metal and (b) 304L EB weld microstructures. R = radial, L = longitudinal.

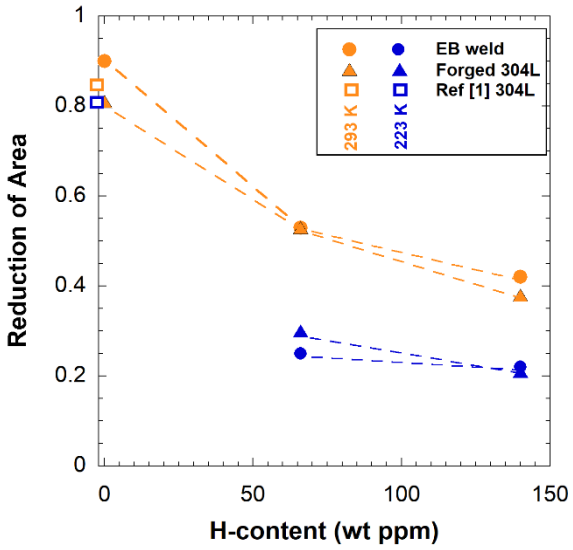

Figure 4. Reduction of area (RA) as function of hydrogen content (wt ppm H) for forged 304L and EB weld at 293 K and 223 K. Open symbols are from forged 304L in Ref [1] and demonstrate negligible change in RA in the absence of hydrogen.

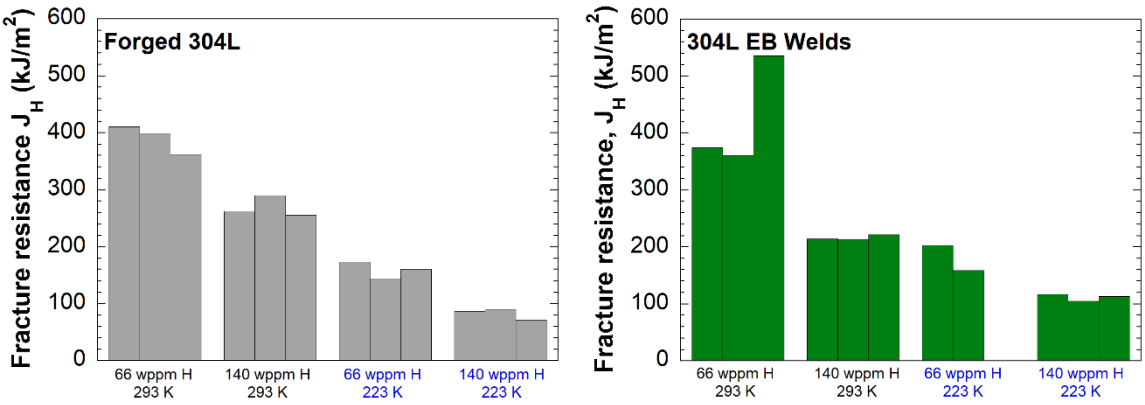

Figure 5. Fracture resistance, J_H, for hydrogen-precharged forged 304L and EB weld arc coupons at 293 and 223 K.

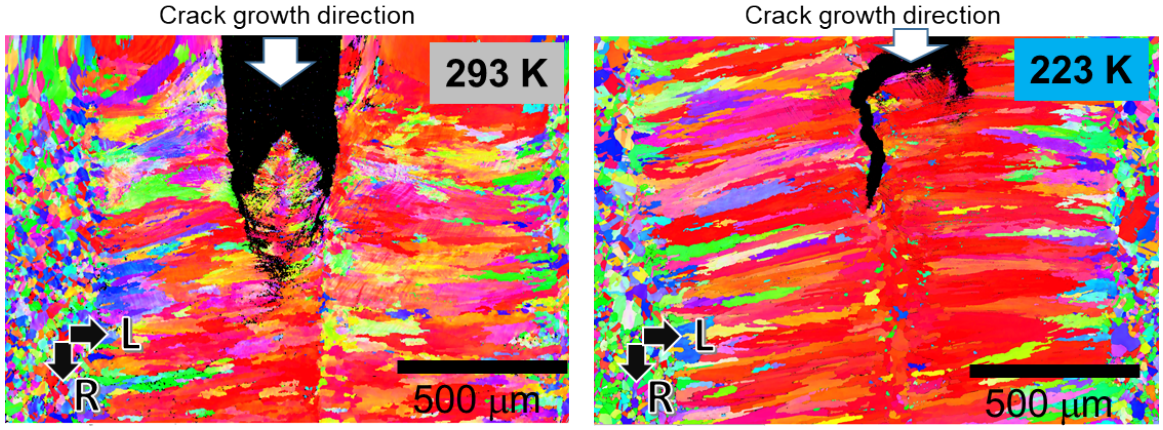

(a) (b)

Figure 6. Electron backscattered diffraction (EBSD) images of crack extension at the end of a fracture test on 304L EB weld fracture test with internal hydrogen content of 140 wt ppm tested at (a) 293 K and (b) 223 K. Crack growth direction is down in both images.

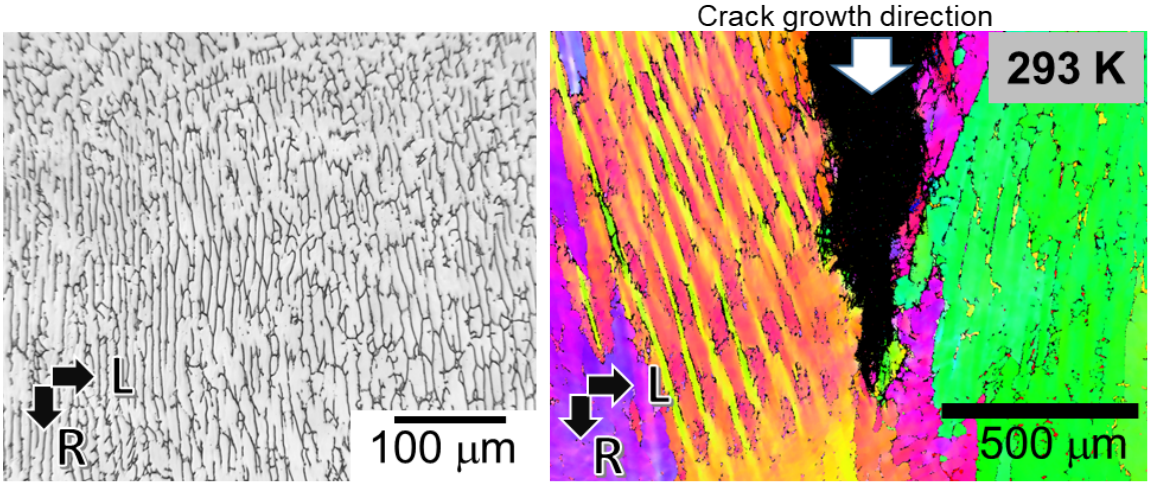

(a) (b)

Figure 7. (a) Optical image of 304L/308L gas tungsten arc weld which was tested in ref [3]. (b) Electron backscattered diffraction (EBSD) image of crack extension at the end of a fracture test on 304L/308L gas tungsten arc weld with internal hydrogen content of 140 wt ppm tested at 293 K. Results from fracture test of 304L/308L were presented in ref [3]. Crack growth direction is down.

Table 1. Tensile properties of Forged 304L

	Temperature (K)	H-content (wt ppm)	YS (Mpa)	UTS (Mpa)	RA
Forged	293	0	447	666	0.81
	293	66	472	701	0.53
	223 (-50°C)	66	412	913	0.30
	293	140	491	742	0.38
	223 (-50°C)	140	433	862	0.21

Table 2. Tensile properties of 304L EB weld

	Temperature (K)	H-content (wt ppm)	YS (Mpa)	UTS (Mpa)	RA
EB weld	293	0	398	605	0.90
	293	66	430	639	0.53
	223 (-50C)	66	463	828	0.25
	293	140	454	672	0.42
	223 (-50C)	140	458	784	0.22

Table 3. Fracture test results of forged 304L and EB weld.

	H-content	Temperature (K)	J_H (kJ/m^2)	Average J_H (kJ/m^2)
Forged 304L	66	293	411	390
			398	
			362	
		223	173	159
			144	
			160	
	140	293	263	270
			290	
			256	
		223	86	82
			90	
			72	
EB Weld	66	293	375	424
			360	
			536	
		223	203	181
			159	
	140	293	214	216
			213	
			222	
		223	117	112
			105	
			113	